Int J Adv Manuf Technol (2017) 91:3349–3361
DOI 10.1007/s00170-017-0019-5

ORIGINAL ARTICLE

Influence of heat treatment on mechanical properties of clinched joints in titanium alloy sheets

Yue Zhang[1] · **Xiaocong He**[1] · **Kai Zeng**[1] · **Lei Lei**[1] · **Fengshou Gu**[2] · **Andrew Ball**[2]

Received: 18 September 2016 / Accepted: 4 January 2017 / Published online: 22 January 2017

Abstract Clinching is a widely used sheet material connection technology in different industrial fields. The effects of annealing and quenching on the mechanical performances of clinched titanium alloy joints were investigated in this research. Tensile–shear tests were carried out to study the join ability, load-bearing capacity, energy absorption, and failure modes of different clinched titanium alloy joints. The F–N curves were obtained from fatigue tests to characterize the fatigue properties of different types of clinched joints. The typical fracture interfaces were analyzed by scanning electron microscopy. Results show that the tensile–shear strength of the clinched titanium alloy joints was severely decreased by quenching, but both tensile–shear strength and energy absorption were improved by annealing. For all types of joints tested, fatigue cracks always appeared near the indentation of the upper sheet. Analysis of the microstructure suggested that the plasticity of the titanium was improved by annealing.

Keywords Clinching · Titanium alloy · Mechanical property · Heat treatment

✉ Xiaocong He
x_he@kmust.edu.cn

[1] Innovative Manufacturing Research Centre, Kunming University of Science and Technology, Kunming 650500, People's Republic of China

[2] Centre for Efficiency and Performance Engineering, University of Huddersfield, Queensgate, Huddersfield HD1 3DH, UK

1 Introduction

Vehicles such as aircraft and cars comprise a large number of mechanical parts produced by a variety of manufacturing processes. Commercial requirements for higher performance, higher productivity, and lower cost in joining operations are becoming more demanding. A trend in manufacturing such products is that both the number of parts and their complexity are increasing, including new combinations of dissimilar materials [1]. However, because of the different melting points and intermetallic compounds formed at the welding interface, it is difficult to join different sheet materials by conventional fusion welding techniques such as resistance welding [2]. Mechanical joining processes were recently developed to solve these problems in fabricating high-performance joints [3]. In recent years, this has resulted in a significant increase in the use of mechanical joining by plastic deformation such as self-piercing riveting (SPR) and clinching in engineering structures and components [4–6]. Clinching is a method of joining sheet metal or extrusions by localized cold forming of materials. The result is an interlocking friction joint between two or more layers of material formed by a punch into a special die [7]. The principle of clinching is given in Fig. 1. Clinching is environmentally friendly due to low-energy requirements, low-noise output, and no fume emissions. It typically involves no heating compared with resistance welding, more efficient in mass production compared to friction stir welding, and has lower production costs if tool service life is guaranteed compared to SPR [8–10].

Previous studies have researched the static and fatigue behavior of clinched joints and the optimization of the parameters in the clinching process, by way of experiments and finite element (FE) analysis. Mucha et al. [11] studied the effect of the clinching process parameters on the join ability of advanced high-strength steel and found that the die groove width

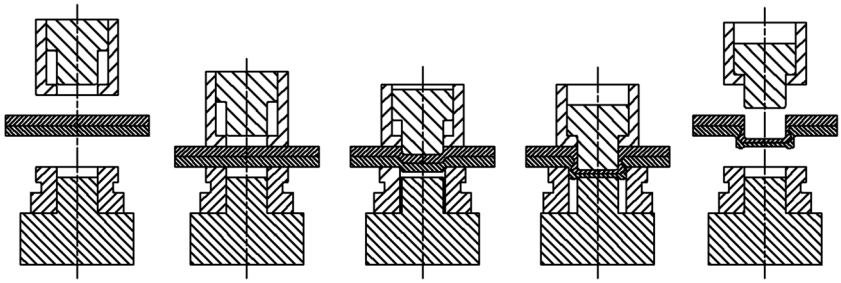

Fig. 1 Principle of mechanical clinching

is the most important parameter affecting the material flow and energy consumption of the joining process. The effect of corrosion phenomena in critical environmental conditions on the mechanical performance of steel/aluminum hybrid clinched joints was studied by aging in salt spray environment [12]. The experimental results have shown that corrosion degradation phenomena significantly affect the performance and failure mechanisms of the joints. A failure map for the joint geometries has been proposed. For describing the evolution of ductile damage, a numerical model was developed by Lambiase and Di Ilio to predict the onset of fracture during the mechanical clinching [13]. An inverse analysis was performed by minimizing the difference between the experimental and numerical prediction concerning the load–stroke curves and the geometries of punched cross sections. The results show that the model enables the onset of cracks in critical regions to be predicted.

Coppieters et al.'s paper [14] deals with the development of an Arcan-like device which enables the introduction of various shear/tensile ratios in clinched joints. An experimental survey of the multi-axial behavior of a non-cutting single-stroke round clinched joint between two DC05 sheets was conducted with this modified Arcan setup. The experimental results were used to check the validity of numerical models that aimed to predict the joint strength under multi-axial loading. In Jiang's paper [15], an electrical resistance method was used to inspect the quality and strength of clinched joints. Results showed that the electrical resistance was more sensitive than the bottom thickness in reflecting the prestraining of the specimens prior to clinching. In Kascak et al.' [16] study, the clinching tool with a die with a specially formed gap and a punch was used for mechanical clinching. Experiments and FE method were applied for the assessment of punch load in the joining process. Mucha et al. [17] presented the pressed joint technology using forming process with or without additional fastener. The capabilities for increasing the load-carrying ability of mechanical joints by applying special rivets and dies were presented. The load-carrying ability of joints was evaluated, and the effect of joint-forming process was compared by measuring the microhardness of the joints. Lee et al. [18] focused on the design method of mechanical clinching tools and indicated that neck thickness and undercut are two significant factors in determining the forming quality. They found that the undercut has a greater impact on joint strength than the neck thickness. In addition, the undercut and the neck thickness are not the only quality parameters for clinched joints. Indeed, the bottom thickness of the joint and the protrusion height have been demonstrated to be highly important [19, 20]. He et al. [21] analyzed the static strengths and energy absorption of clinched joints and clinching-bonded hybrid joints by using a FE method and supporting experiments. Mori et al. [22] compared the static and fatigue strengths of mechanically clinched, SPR joints and resistance spot-welded joints in aluminum alloy sheets, and the fatigue behavior of mechanical clinching exhibited values in the middle of the range. Carboni et al. [23] studied the influence of load direction on the joint strength of transverse joints and longitudinal joints. The joint configuration was found not to be significant. Wen et al. [24] developed a new clinching method called flat hole-clinching (FHC) that is suitable for assembling two layers of sheet materials without protrusion at the joints. Al 6063 and AZ31 plates with thicknesses of 0.8 and 1.0 mm were employed in the experiment and numerical simulation to examine the impact of tool and hole geometries, material properties, and relative thicknesses on joints. The results confirmed that various combinations of sheet materials can be connected reliably by FHC, with even higher joining strengths in comparison to conventional clinching.

Recently, the trend of the clinching development is becoming more flexible. A compressing technology was investigated by Chen et al. [25] in order to reduce the protrusion height. A pair of dies was used to compress the protrusion in a single stroke. The interlock and neck thickness were enlarged with the decrease of the protrusion height in the compressing process. Chen et al. [26] also proposed a height-reducing method. Flat dies were used to conduct the height-reducing process in the experiment. A rivet was used in the height-reducing process to control the material flow of the protrusion and increase the strength of the joint. Results show that the method was effective for reducing the protrusion height and increasing the

Table 1 Chemical compositions of TA1 material (%)

Material	Fe	Si	C	N	H	O	Ti
TA1	0.15	0.1	0.05	0.03	0.015	0.15	–

Table 2 Mechanical property of TA1 material

Material	Tensile strength (MPa)	Yield strength (MPa)	Young's modulus (GPa)	Elongation (%)
TA1	430.5	396.8	98.5	33

strength of the joint produced with different sheets. In Lee et al.'s study [27], a new hole-clinching process was developed for joining high-strength material to ductile material. The hole-clinching tools were designed based on the geometrical relationship between the forming volume and the joint strength. FE analysis and practical experiments were performed to verify the practicality of the hole-clinching process. Gibmeier et al. [28] used the diffraction methods for the determination of characteristic residual stress (RS) distributions in undismantled clinched samples for the assessment of the influence of RS on the mechanical behavior of clinched joints. Results show that the combined RS determination by X-ray and neutron diffraction can be used to obtain an expressive assessment of the RS distributions in the immediate vicinity of clinched joints. The join ability of aluminum alloy sheets with reduced ductility produced by mechanical clinching is analyzed by Lambiase et al. [29]. A modified tool set geometry was developed to reduce the localization and magnitude of plastic strain. Sheet preheating was adopted to increase the material formability. Mechanical characterization tests were conducted to evaluate the influence of the processing conditions on joint strength.

The studies discussed above were conducted on many metals such as steel, aluminum, or copper alloy. On the other hand, recent developments have dealt with low-ductility materials such as magnesium, titanium alloys along with hybrid joints involving metals and thermoplastic polymers. Tests on joints using these materials have so far always cracked at the neck or at the bottom of the button of the clinched joints. Trials aimed at overcoming these weakness trials have been conducted. Neugebauer et al. [30] studied the effect of preheating when joining thin magnesium sheets, using a flat die heated by a resistive cartridge with very short process times. Results showed that the development of cracks could be stopped by preheating the sheets before joining to increase the material formability. Lambiase et al. [31, 32] investigated how the material flow can be controlled by a combination of preheating and modified tool geometry. They determined suitable joining conditions (geometry of the clinching tools and preheating) for joining thicker PMMA, PC, and PS sheet with aluminum sheets. The suitability of mechanical clinching to join fiber-reinforced plastics with aluminum sheets was investigated by Lambiase et al. [33]. The influence of sheet thickness and alloy composition on join ability and mechanical behavior of the joints was analyzed. Geometry evolution of the joints during clinch joining was studied to understand the material flow and damage evolution of both aluminum and glass fiber reinforced polymer (GFRP) sheets.

Titanium alloys have been widely used in the automobile industry and aerospace industry in recent years [34]. Titanium alloy has advantages such as high strength, corrosion resistance, and thermostability. It can be used in aircraft body, heat exchanger and corrosion-resistant structures, and so on [35]. In the previous paper by He et al. [36], the static behavior of extensible die clinched joints in titanium sheet materials was investigated. An oxyacetylene flame gun was used to heat up titanium thin sheets up to 700 °C before clinching. The static mechanical properties and failure modes of clinched joints in different titanium sheets were studied. However, no investigation of the fatigue properties of clinched joints in titanium alloys has been published until now. In the present study, the effects of annealing and quenching on the fatigue performance of clinched titanium alloy joints were investigated. Tensile–shear tests were carried out to study the load-bearing capacity, energy absorption, and failure modes of different clinched joints in titanium alloy. Fatigue load–fatigue life curves were obtained via tension–tension fatigue tests to characterize the fatigue properties of the clinched joints. The typical fracture interfaces were analyzed by scanning electron microscopy (SEM). The results show that annealed and untreated clinch joints in titanium alloy have different advantages and disadvantages and should be used to satisfy different requirements in practical applications.

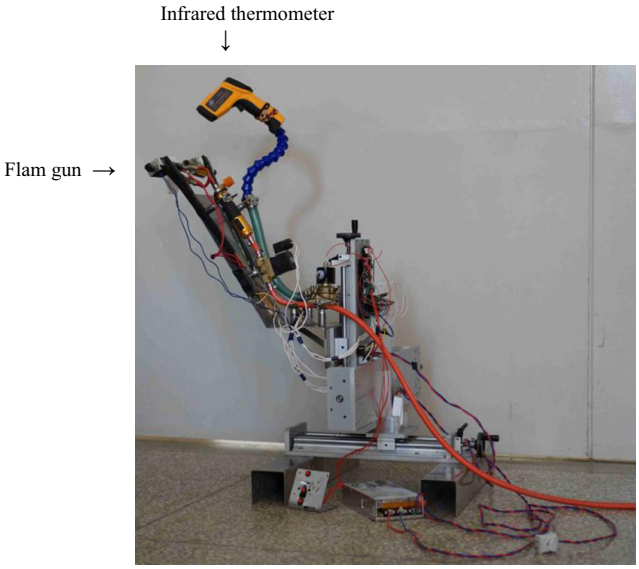

Fig. 2 Heating platform

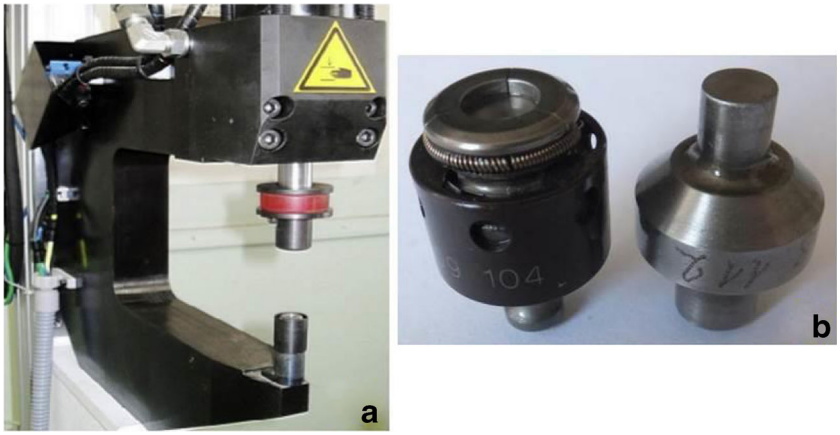

Fig. 3 Clinching machine and extensible die clinching tools

2 Specimen preparation and heat treatment procedure

2.1 Sheet material

The materials used in this study were TA1 titanium alloy (TA1) sheets with the dimensions 110 mm length × 20 mm width × 1.5 mm thickness. All sheets were cut along the rolling direction. The chemical compositions and the mechanical properties of the TA1 sheet materials are listed in Tables 1 and 2 separately.

2.2 Specimen preparation

It is difficult to join TA1 sheets because of the limited deformation properties of TA1 materials at room temperature. For easy clinching, TA1 titanium sheets were preheated locally to 700 °C by an oxyacetylene flame gun as shown in Fig. 2. The heating temperature can be controlled by an infrared thermometer. The clinching processes were produced immediately after heat treatment.

A RIVCLINCH 1106 P50 system was used as the clinching machine. The clinching machine and one set of the extensible die clinching tools are shown in Fig. 3. Both the punch (serial number 3924738112) and the flat-bottom extensible die (serial number 39242709104) are made of high-strength steel. The diameter of the punch is 5.7 mm; the fillet radius of the punch is 0.7 mm. The cavity depth of the extensible die is 1.4 mm. Clinched specimens consist of two thin TA1 sheets (110 × 20 × 1.5 mm), and the overlap of the two sheets was 20 mm, as shown in Fig. 4. The fixed forming force used in preparing the test samples was determined on the basis

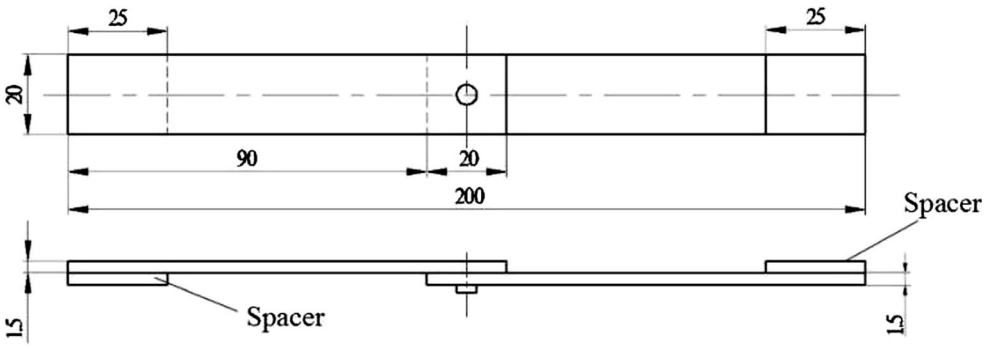

Fig. 4 Specimen configuration and boundary condition of a clinched joint (dimensions in millimeter)

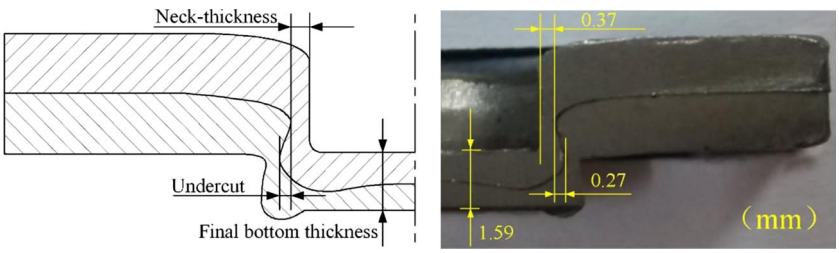

(a) Clinching quality assessment criteria (b) Typical cross-section of clinched joint

Fig. 5 Clinched joint quality assessment

Fig. 6 RX3-30-9 industrial furnace

of preliminary tests to guarantee qualified clinching. All clinched joints were formed with equal bottom thickness, controlled by the stroke of the punch.

Clinched joint quality can be assessed by three criteria, the neck thickness, the undercut, and the final bottom thickness as shown in Fig. 5a. A specimen was cut from the centerline of the indentation, perpendicular to the length of the specimen. The typical cross section of clinched joint in TA1 sheet material is shown in Fig. 5b. The average neck thickness is 0.37 mm; the average undercut is 0.27 mm, and the average final bottom thickness is 1.59 mm. It is clear that the TA1 sheet material can form a good interlock by mechanical clinching.

2.3 Heat treatment procedure

It is generally known that the relief annealing can remove the residual stress after the deformation processing without changing the microstructure. Consequently, it will stabilize the size and the shape of the work pieces and reduce the tendency of deformation as well as cracking of the parts in the process of using. In addition, the microstructure and properties of the material can be changed by quenching treatment, which can improve the strength, hardness, and toughness of the material [37]. In order to investigate the influence of heat treatment on mechanical properties of clinched joints in titanium alloy sheets, the test specimens were divided equally into three groups for further study. Each group has at least 20 specimens: 10 specimens for tensile shear test, 9 specimens for fatigue test, and 1 specimen for metallographic structure and microhardness tests. One group of specimens was annealed after heating, and another group was quenched. The annealing experiments and quenching experiments were conducted in an RX3-30-9 industrial furnace, as shown in Fig. 6.

It is known that the stress relief annealing temperature of TA1 ranges between 480 and 595 °C, keeping a certain time between 0.25 and 4 h. In addition, TA1 belongs to the alpha phase of titanium alloy, and the beta phase transition temperature is between 890 and 920 °C [37]. In the present study, the annealing temperature and keeping time were selected as 540 °C and 1 h. The quenching temperature and keeping time were selected as 900 °C and 5 min. The heat treatment temperature can be controlled by the temperature control system

Table 3 Heat treatments of clinched joints in titanium alloy sheets

Name of the specimens	Heat treatment method	Heating temperature	Heat-up time	Cooling medium	Cooling time
CT	Untreated	This group of the specimens was subjected to no disposal.			
ACT	Annealing treatment	540 °C	1 h	Air	Up to room temperature
QCT	Quenching treatment	900 °C	5 min	Water	Up to room temperature

Table 4 Mean load and confidence intervals of three types of clinched joints

Clinched joints	Mean load/N	Standard deviation	Variable coefficient	Confidence interval of 95%	Mean displacement/mm
CT	4360	121.11	0.0278	4126.28, 4601.05	1.48
ACT	3880	175.58	0.0453	3535.60, 4233.88	1.85
QCT	3500	168.31	0.0482	3160.45, 4150.12	0.83

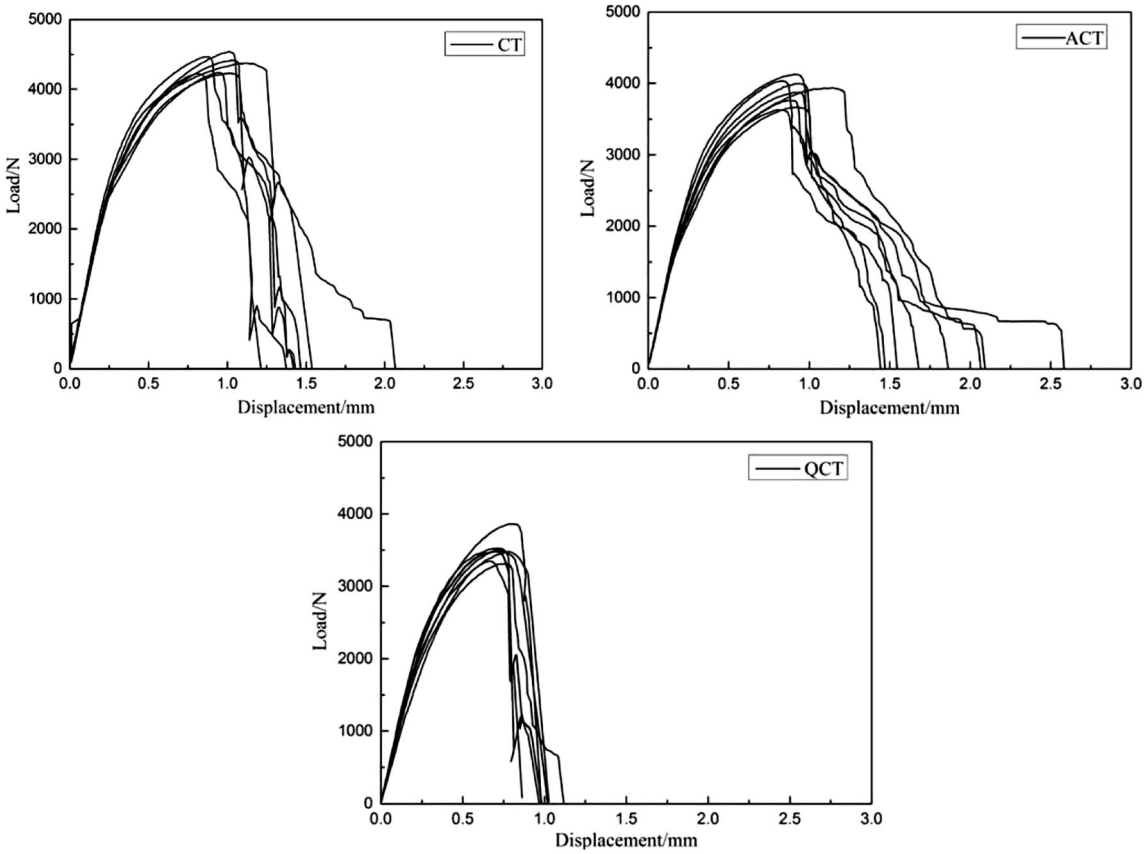

Fig. 7 Load–displacement curves of three types of clinched joints

mounted in the RX3-30-9 industrial furnace. The clinched joints and the annealing and quenching process are summarized in Table 3.

3 Tensile–shear tests and result discussion

3.1 Tensile–shear tests

An MTS Landmark100 servo-hydraulic testing machine with hydraulic grips was used to conduct tensile–shear tests of clinched joints. The tests were executed at a speed of 5 mm/min, under the displacement control mode in order to characterize the static behavior of the joints. Spacers were used to minimize bending effects during the tests, as shown in Fig. 4.

The mean values of the ultimate loads and the failure displacements after tensile–shear test are shown in Table 4. The load–displacement curves of different clinched joints are shown in Fig. 7. To enable easy comparison, all load–displacement curves of different clinched joints were drawn in the same coordinate scales. The tensile–shear strength of the ACT was reduced by 10.4%, and the failure displacement increased by 25% compared with the results for the CT samples. The tensile–shear strengths and failure displacements of the QCT samples were significantly worse than the values

Fig. 8 Failure modes after tensile–shear tests

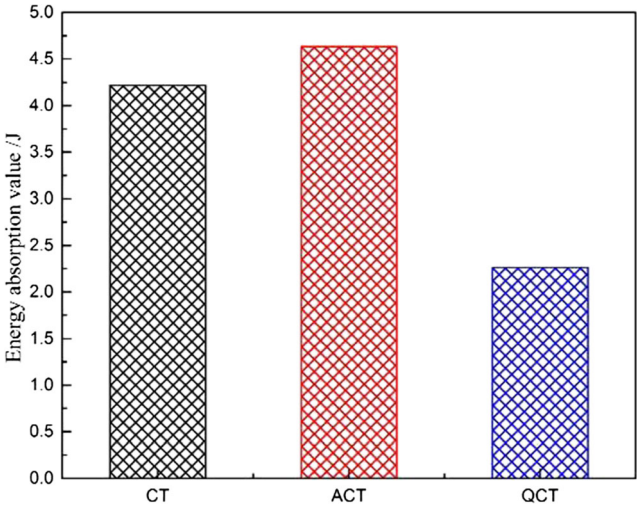

Fig. 9 Energy absorption value of clinched joints

obtained for the CT samples. This strongly suggests that quenching treatment does not improve the performance of clinched joints of the TA1 material.

Figure 8 shows the failure modes of the three types of clinched joints. There is widespread agreement among researchers that failure modes after tensile–shear test of the clinched joints can be divided into three types: fracture of the upper sheet at the neck where the material is thinnest, pull-out of the upper sheet resulting in its separation from the bottom sheet, and mixed failure with evidence of fracture and pull-out occurring simultaneously [19, 20]. In this research, all test samples subjected to tensile–shear loads eventually failed as a result of neck fractures followed by the upper sheet separating from the lower sheet. Under the tensile–shear load, the neck of the upper sheet bears a main shear load by geometrical interlocking. When the shear stress reaches the yield criterion of TA1 sheet material, a crack is initiated from the interfacial surface of the upper sheet and grows into the upper sheet thickness. After rowing into the upper sheet, crack kinks toward the button center and then propagates along the circumference of the button neck of the upper sheet. Finally, the inner button is sheared off at the neck. Moreover, as shown in Fig. 7, the tensile–shear strength of the CT samples decreased sharply after reaching the peak load. This indicated that in each case, the crack propagated rapidly and fractured immediately. On the other hand, the tensile–shear strength of the ACT samples decreased gently after reaching the peak load. It can be inferred, therefore, that the plasticity of the material had been improved by annealing.

Mechanical clinching has found applications in heavy-duty situation, such as car bodies. Besides load-bearing capacity, energy absorption is an important feature of clinched joints. Energy absorption can be calculated as the area underlying the force–displacement curve. Figure 9 shows the energy absorption of the three types of clinched joints. The energy absorption of CT is 4.22 J; the standard deviation is 0.19. The energy absorption of ACT joint was higher by 9.7%, but the energy absorption of QCT was lower by 46%.

Plastic deformation occurred prior to abrupt failure when the plastic material was subjected to increased force, and consequently, the annealed joints had better performance in plastic deformation and energy absorption. The subsequent analysis focused on the CT and ACT because they have superior static behaviors.

3.2 Result discussion

To further analyze the influence of annealing treatment on clinched joints, CT joint and ACT joint were cut along the axial direction. The Kroll etching agent was used to corrode the surface of the specimens. The volume ratio of the etching agent was $HF/HNO_3/H_2O$ = 1:2:47. A Nikon ECIPSE MA200 microscope was employed to observe the metallographic structure. Figure 10 shows the metallographic structure of CT and ACT clinched joints with magnification of ×200. As can be seen from Fig. 10, the metallographic structure of the untreated TA1 and annealed TA1 is all presented with equal axis alpha phase. The metallographic structure of the equal axis alpha phase is close-packed hexagonal structure, which has strong ability to resist plastic deformation and strong anisotropy. It can be inferred that the stress annealing has little effect on the microstructure of TA1 sheet material but reduced

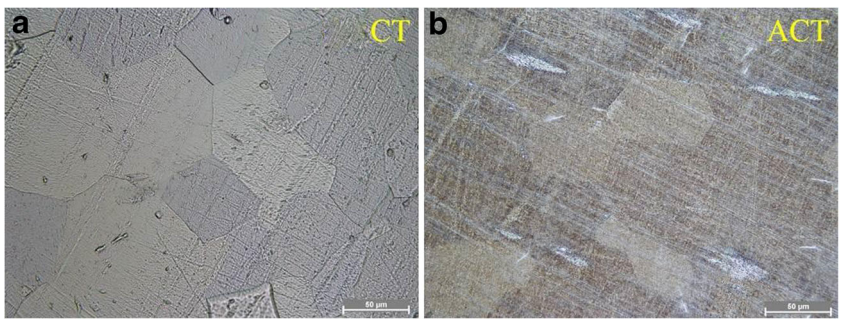

Fig. 10 Metallographic structure of CT and ACT clinched joints

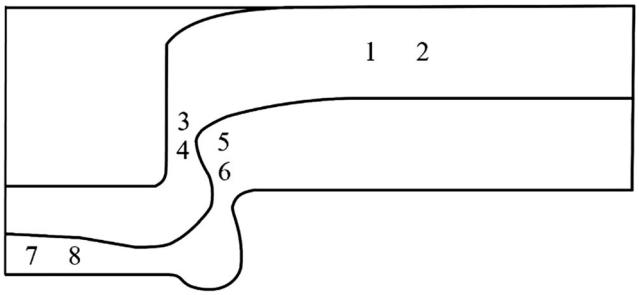

Fig. 11 Schematic of the typical locations for microhardness tests

the residual stress and made the size and shape of the specimen more stable.

The microhardness tests of the CT joint and ACT joint were also carried out. Taking advantage of the symmetry of the clinched joints, the microhardness tests were performed on the half of the joint. As illustrated in Fig. 11, four typical locations on the joint were selected and numbered. These four typical locations include undeformed zone (points 1 and 2), large plastic deformation zone (points 3, 4, 5, and 6), and sheet–die contacted zone (points 7 and 8). The microhardness of each point of the CT joints and ACT joints was detected by a microhardness tester. The microhardness of each point is listed in Table 5. Results show that the average microhardness of the CT joint is 146.68 HV and the average microhardness of the ACT joint is 151.09 HV. That means that the microhardness was increased by 3% due to the stress relief annealing. As a plastic processing technology, the cinching process will result in cold hardening of the metal sheets. However, relief annealing can remove the residual stress without changing the microstructure and lead to microhardness increase which improve the energy absorption of the clinched joints in titanium alloy sheets.

4 Fatigue analysis

4.1 Fatigue tests

The parameters to be used in the fatigue tests were determined on the basis of the average peak load obtained from the static tests. Load-controlled cyclic tension–tension fatigue tests were conducted on test specimens using an MTS servo-hydraulic testing machine, employing a sinusoidal waveform with the load ratio $R = 0.1$ and frequency $f = 20$ Hz. A specimen was considered broken when the two sheets separated or the number of cycles had reached two million. Three different fatigue load levels were used to obtain the fatigue behaviors of the CT and ACT samples because fatigue lives are usually divided into short life, medium life, and long life areas. At least three tests were performed for each load level.

The fatigue life and failure modes are listed in Table 6. There were four different failure modes evident following the fatigue tests. To aid discussion of the failure modes, the following nomenclature is used here:

Failure mode I: neck fracture with spindle-shaped crack near the indentation of the upper sheet.
Failure mode II: neck fracture with the upper sheet almost broken near the indentation.
Failure mode III: the upper sheet broken near the indentation.
Failure mode IV: the cycle number reached two million with no visible joint failure.

Figure 12 shows different failure modes for the clinched joints. With reference to Table 6, the images in Fig. 12 show that the fatigue failure mode caused by the high amplitude load was similar to that found in the tensile tests. When the stress amplitude is great, the most fragile part of a clinched

Table 5 Microhardness of the CT joint and ACT joint

Specimens/points	1	2	3	4	5	6	7	8	Mean value/HV	Standard deviation
CT	158.2	142.9	136.7	128.1	142	144.7	173.7	147.1	146.68	13.88
ACT	113.5	127.7	195.9	198.1	174.9	183.9	214.7	184.6	151.09	35.32

Table 6 Fatigue lives and failure modes of CT and ACT joints

	Maximum load/kN (load level)	Fatigue life	Failure modes
CT	2.618 (60%)	99,629, 220,378, 98,906	I, I, II
	2.182 (50%)	459,748, 695,827, 770,643	II, II, II
	2.007 (46%)	1,236,903, 813,166, 771,261	III, II, III
ACT	2.328 (60%)	48,040, 100,807, 60,892	I, I, I
	2.182 (45%)	304,386, 366,751, 414,893	II, II, II
	2.007 (33%)	1,124,511, 2,000,000, 2,000,000	II, IV, IV

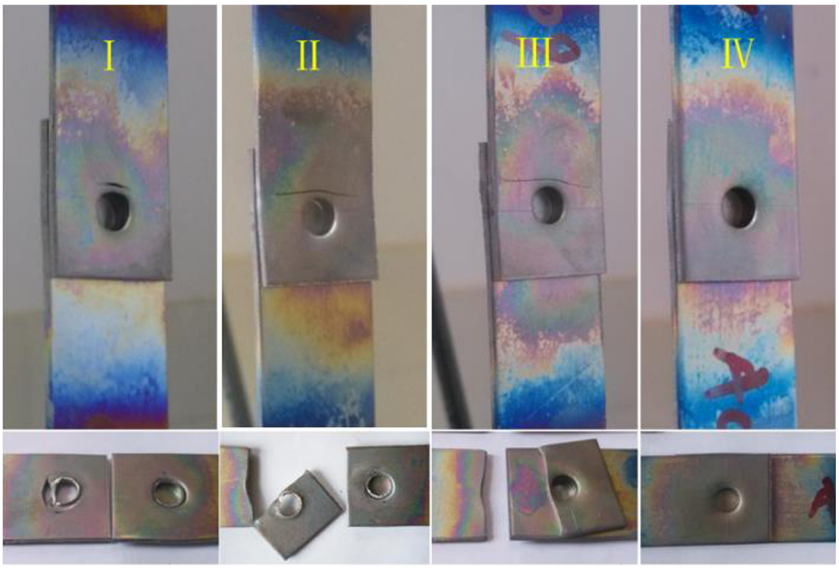

Fig. 12 Different failure modes of the clinched joints

joint is the neck, where the material is thinnest. However, when the load amplitude is less, then the failure mode changes to the neck fracture and upper sheet fracture. The vulnerable location is the neck of the joint near the indentation of the upper sheet. Smaller load stress amplitudes lead to an upper sheet fracture with the cracks appearing near the indentation, with the upper sheet breaking up before the neck fracture appears. Very little damage occurred on the specimens when the load amplitude was lower than the fatigue limit.

4.2 Results and discussion

The values for fatigue load-fatigue life (F–N) were plotted on single logarithmic coordinates and curves fitted by the least squares method (LSM), as shown in Fig. 13. Two parameters of the power function formula of middle life range can be presented as

$$S^m N = C \tag{1}$$

where S is the amplitude of the stress and N denotes the fatigue life. C and m are undetermined coefficients based on the categories of structural component.

Taking the logarithm on both sides of the equation

$$\log N = \log C - m \log S \tag{2}$$

Make $\log N = Y$, $\log C = A$, $-m = B$, and $\log S = X$, and Eq. (2) is simplified as

$$Y = A + BX \tag{3}$$

The least squares method is used to fit Eq. (3), and the regression equations of F–N curve at single logarithmic coordinate system are

$$Y_{CT} = 5.7887 - 0.6258X \tag{4}$$

$$Y_{ACT} = 5.8020 - 0.7261X \tag{5}$$

The two parameters power function of the two kinds of joints are

$$N_{CT} = 10^{5.7887} S^{-0.6258} \; C_{CT} = 10^{5.7887} \; m_{CT} = 0.6258 \tag{6}$$

$$N_{ACT} = 10^{5.8020} S^{-0.7262} \; C_{ACT} = 10^{5.8020} \; m_{ACT} = 0.7262 \tag{7}$$

With increasing number of cycles, the load amplitude decreases. The absolute slopes of the F–N curves for CT and ACT samples are about 0.63 and 0.73, respectively. The fatigue limit for the CT samples is nearly 1.9 kN, and for the

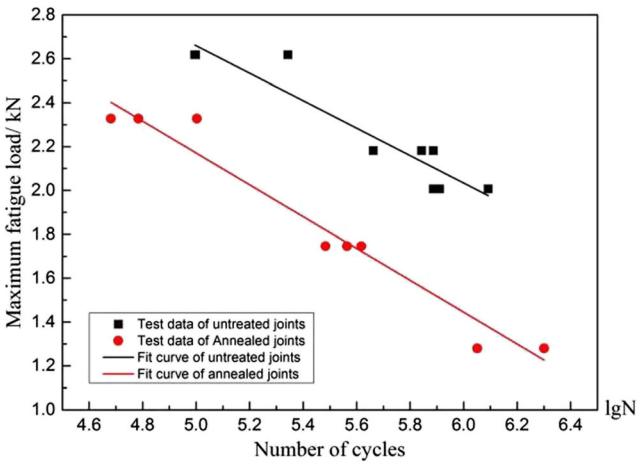

Fig. 13 F–N curves of CT and ACT joints

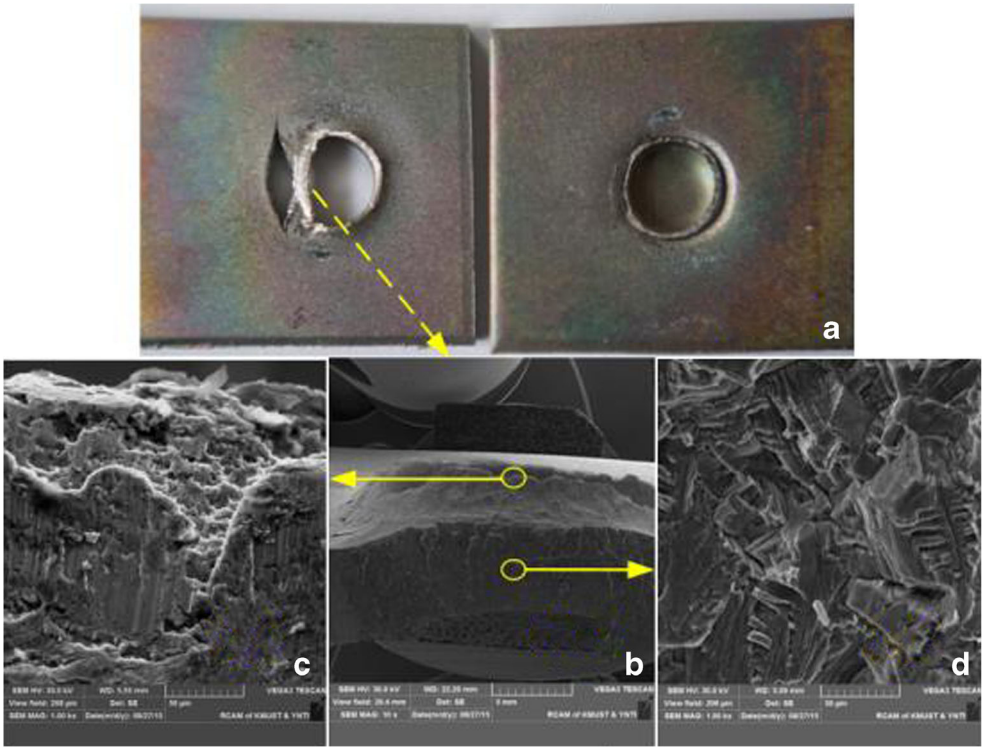

Fig. 14 SEM analysis of CT at a high load stress amplitude

ACT samples, the fatigue limit is nearly 1.3 kN. It is obvious that the fatigue property of the TA1 clinched joints was superior to that of annealed ACT samples, with the fatigue strength of the CT samples 68% higher than for the ACT samples. That is because the TA1 material was in the metastable state and the crystal lattice was distorted after cold deformation (mechanical clinching). Flaws and dislocations were induced in the internal crystal lattice resulting in a rise of distortion energy. The annealing process can promote recuperation of the point defect and dislocation motion in

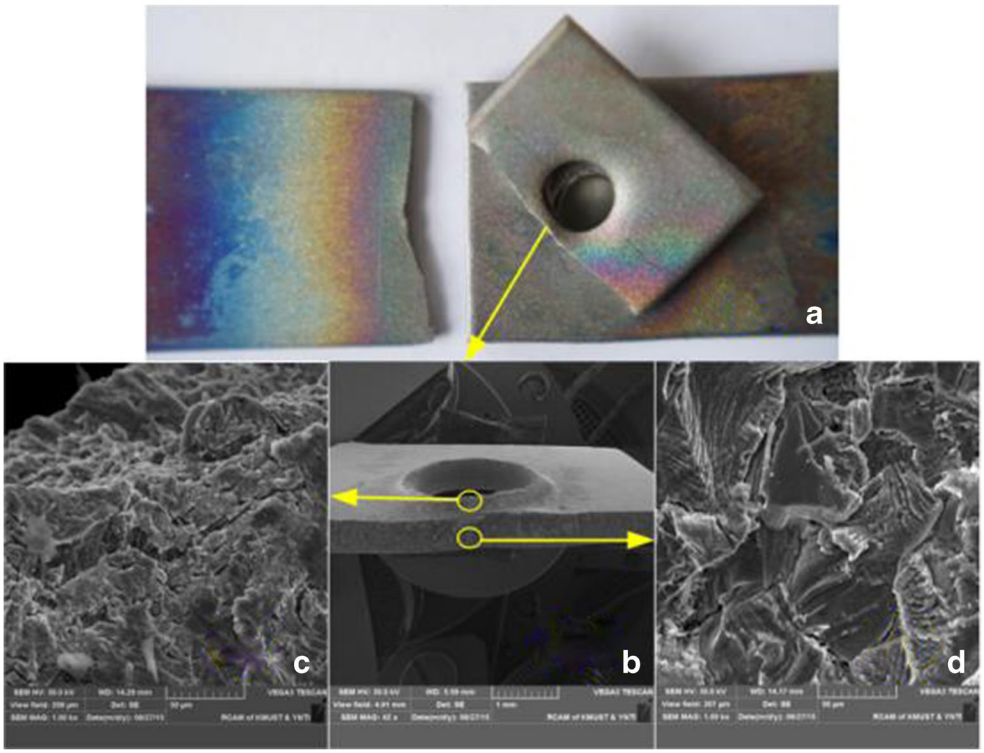

Fig. 15 SEM analysis of CT at a low load stress amplitude

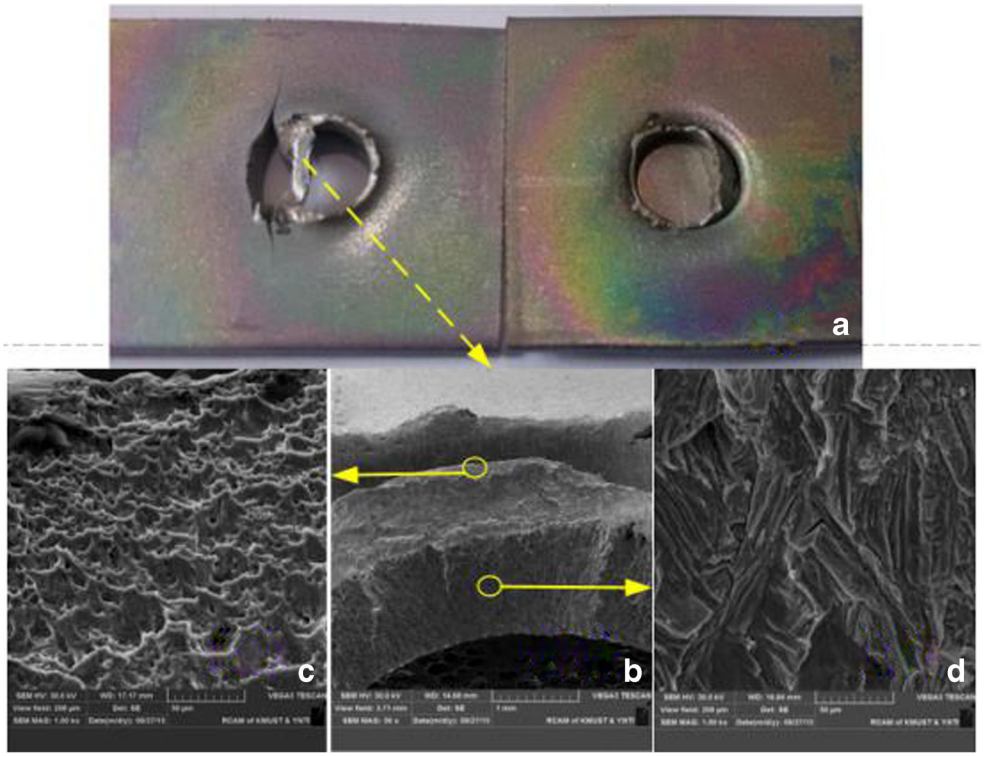

Fig. 16 SEM analysis of ACT at a high load stress amplitude

the titanium crystal lattice, releasing energy and increasing the plasticity of the material. Usually, the strength of the material exhibits an inverse relationship with the plasticity of the material. Improving the plasticity leads to a decrease in strength. This is also reflected in the results of the tensile tests. Therefore, whether to anneal the TA1 clinched joints or not depends on the operating conditions in practical applications.

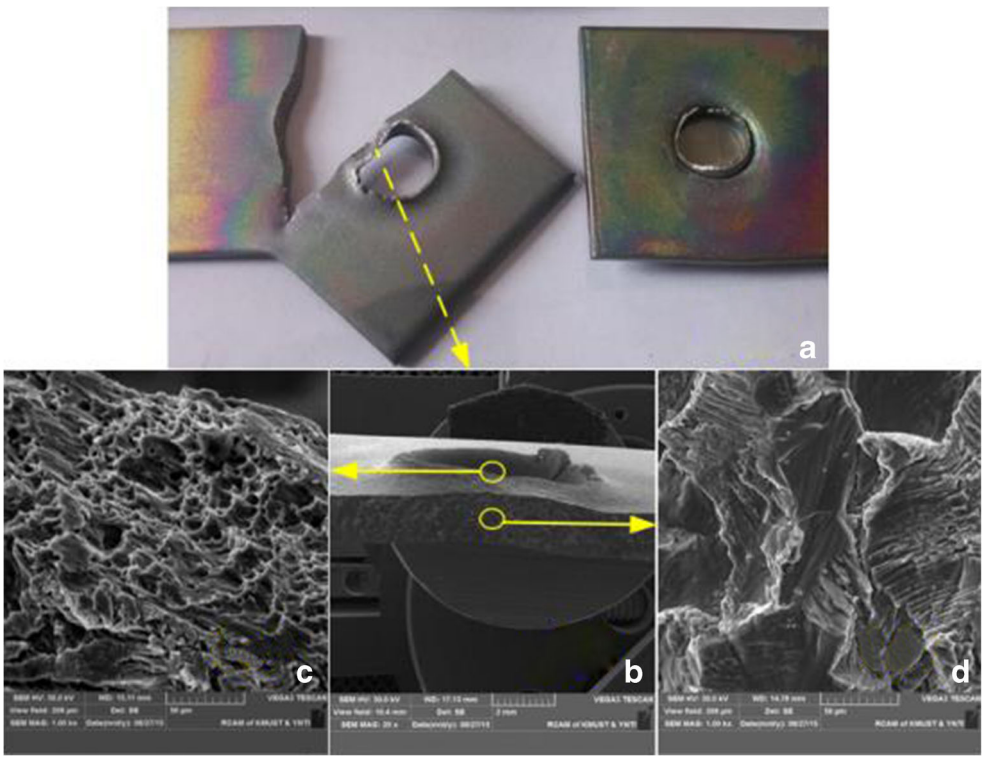

Fig. 17 SEM analysis of ACT at a low load stress amplitude

4.3 Microstructure analysis

The fracture surfaces of the failed specimens were examined directly in a VEGA3 SCAN SEM system without any further preparation. Comparisons were made between the corresponding fatigue fracture areas of the CT and ACT samples. Figures 14 and 15 are the SEM analysis pictures of the CT samples. Figures 16 and 17 are the SEM pictures of the ACT samples. All four pictures were arranged as follows:

Image (a) shows the fatigue failure of the joints.
Image (b) shows the fracture at low magnification.
Image (c) shows the neck fracture at higher magnification.
Image (d) is a magnified view of the fatigue source region.

Figures 14d and 15d show multi-series of irregular fatigue striations perpendicular to the direction of local crack propagation. It can be inferred that stress was concentrated in this region (near the indentation of the upper sheet) and that fatigue cracks originated there. There are many terraces with altitude intercepts shown in Fig. 14d. These were caused by propagation from multiple fatigue sources. In Fig. 15d, the fatigue striations are narrower because the load stress amplitude decreased. There are crystallographic planes and fan-shaped desert lines in that location. It is a brittle fatigue fracture and indicates a slow propagation rate for the crack.

In Fig. 16d, the altitude intercepts of fatigue terraces are lower than in Fig. 14d, though they were all produced under high amplitude load stress. The crack surface has the features of cleavage transgranular fracture and hydrogen embrittlement. That is because elemental hydrogen dissolved in the titanium when the substrates (upper and lower sheets) were heated in the air before the clinching process, and they aggregated into hydrogen molecules which resulted in stress concentration.

There are fewer, wider fatigue striations in Fig. 17d compared to Fig. 15d though they were all produced under low load stress amplitude. When it comes to the ACT samples, many small, equally sized dimples appeared at the neck fracture, as shown in Figs. 16c and 17c. The shape and size of the dimples suggested that the sheet materials in those regions suffered tensile fracture. This, in turn, suggested that the plasticity of the material was enhanced by the annealing treatment. This is consistent with the conclusion reached in Sect. 4.2 above.

5 Conclusions

This paper contributes to basic studies on the static mechanical properties and fatigue behavior of clinched joints in titanium sheets. The clinching processes and failure modes of the clinched joints were investigated experimentally. The main results of the work are as follows:

1. Mechanical clinching can be used to join titanium sheets. The clinched joints have good join ability and load-bearing capacity.
2. The fatigue limits of the CT and ACT samples were 1.9 and 1.3 kN, respectively. The fatigue strength of the CT samples was 68% higher than for the ACT samples. The fatigue strength of the CT joint is superior to that of ACT joint.
3. The fatigue cracks in the CT and ACT samples always occurred in the upper sheet. Microstructure analysis suggested that stress concentration and fatigue sources appeared near the indentation and are brittle fatigue fractures. However, the neck fractures in the ACT samples were ductile fractures.
4. The plasticity and energy absorption of the clinched joints were enhanced by annealing treatment, but the tensile strength and fatigue strength were decreased.

Acknowledgements This study is supported by the National Natural Science Foundation of China (Grant No. 51565023) and Major Program Foundation of the Education Department of Yunnan Province, China (Grant No. ZD201504).

References

1. Mori K, Bay N, Fratini L, Micari F, Tekkaya A (2013) Joining by plastic deformation. CIRP Annals – Manuf Technol 62(2):673–694
2. He X (2012) Finite element analysis of laser welding: a state of art review. Mater Manuf Process 27:1354–1365
3. Groche P, Wohletz S, Brenneis M, Pabst C, Resch F (2014) Joining by forming—a review on joint mechanisms, applications and future trends. J Mater Process Technol 10:1972–1994
4. Mucha J (2015) The failure mechanics analysis of the solid self-piercing riveting joints. Eng Fail Anal 47(PA):77–88
5. Eshtayeh MM, Hrairi M, Mohiuddin AKM (2016) Clinching process for joining dissimilar materials: state of the art. Int J Adv Manuf Technol 82(1–4):179–195
6. He X, Liu F, Xing B, Yang H, Wang Y, Gu F, Ball A (2014) Numerical and experimental investigations of extensible die clinching. Int J Adv Manuf Technol 74(9–12):1229–1236
7. Jiang T, Liu ZX, Wang PC (2014) Effect of aluminum pre-straining on strength of clinched galvanized SAE1004 steel-to-AA6111-T4 aluminum. J Mater Process Technol 215:193–204
8. Pinger T, Ruckriem EM (2016) Investigation on the corrosion and mechanical behavior of thin film batch galvanized thick plate components in clinch joints. Int J Adv Manuf Technol 86(1–4):29–36
9. Calabrese L, Galtieri G, Borsellino C, Di Bella G, Proverbio E (2016) Durability of hybrid clinch-bonded steel/aluminum joints in salt spray environment. Int J Adv Manuf Technol 87(9–12): 3137–3147
10. He X, Xing B, Zeng K, Gu F, Ball A (2013) Numerical and experimental investigations of self-piercing riveting. Int J Adv Manuf Technol 69(1–4):715–721

11. Mucha J (2011) The analysis of lock forming mechanism in the clinching joint. Mater Des 32(10):4943–4954
12. Calabrese L, Proverbio E, Galtieri G, Borsellino C (2015) Effect of corrosion degradation on failure mechanisms of aluminium/steel clinched joints. Mater Des 87:473–481
13. Lambiase F, Di Ilio A (2016) Damage analysis in mechanical clinching: experimental and numerical study. J Mater Process Technol 230:109–120
14. Coppieters S, Lava P, Van Hecke R, Cooreman S, Sol H, Van Houtte P, Debruyne D (2013) Numerical and experimental study of the multi-axial quasi-static strength of clinched connections. Int J Mater Form 6(4):437–451
15. Jiang T, Liu ZX, Wang PC (2015) Quality inspection of clinched joints of steel and aluminum. Int J Adv Manuf Technol 76(5–8): 1393–1402
16. Kascak L, Spisak E, Kubik R, Mucha J (2016) FEM analysis of clinching tool load in a joint of dual-phase steels. Strength Mater 10:1–7
17. Mucha J, Kascak L, Spisak E (2013) The experimental analysis of forming and strength of clinch riveting sheet metal joint made of different materials. Adv Mech Eng. doi:10.1155/2013/848973
18. Lee C, Kim J, Lee S, Ko D, Kim B (2010) Design of mechanical clinching tools for joining of aluminum alloy sheets. Mater Des 31(4):1854–1861
19. Lambiase F, Ko DC (2016) Feasibility of mechanical clinching for joining aluminum AA6082-T6 and carbon fiber reinforced polymer sheets. Mater Des 107(10):341–352
20. Lambiase F (2015) Mechanical behaviour of polymer-metal hybrid joints produced by clinching using different tools. Mater Des 87(12):606–618
21. He X, Zhao L, Yang H, Xing B, Wang Y, Deng C, Gu F, Ball A (2014) Investigations of strength and energy absorption of clinched joints. Comput Mater Sci 94:58–65
22. Mori K, Abe Y, Kato T (2012) Mechanism of superiority of fatigue strength for aluminum alloy sheets joined by mechanical clinching and self-pierce riveting. J Mater Process Technol 212:1900–1905
23. Carboni M, Beretta S, Monno M (2006) Fatigue behavior of tensile-shear loaded clinched joints. Eng Fract Mech 73:178–190
24. Wen T, Huang Q, Liu Q, Ou WX, Zhang S (2016) Joining different metallic sheets without protrusion by flat hole clinching process. Int J Adv Manuf Technol 85(1–4):217–225
25. Chen C, Zhao S, Cui M (2016) An experimental study on the compressing process for joining Al6061 sheets. Thin-Wall Struct 108(11):56–63
26. Chen C, Zhao S, Han X (2016) Investigation of the height-reducing method for clinched joint with AL5052 and AL6061. Int J Adv Manuf Technol. doi:10.1007/s00170-016-9266-0
27. Lee C, Lee J, Ryu H (2015) Design of hole-clinching process for joining of dissimilar materials –Al6061-T4 alloy with DP780 steel, hot-pressed 22MnB5 steel, and carbon fiber reinforced plastic. J Mater Process Technol 214(10):2169–2178
28. Gibmeier J, Rode N, Lin R, Oden M, Scholtes B (2002) Residual stress in clinched joints of metals. Appl Phys A Mater Sci Process 74(12):S1440–S1442
29. Lambiase F, Di Ilio A, Paoletti A (2015) Joining aluminium alloys with reduced ductility by mechanical clinching. Int J Adv Manuf Technol 77(5–8):1295–1304
30. Neugebauer R, Kraus C, Dietrich S (2008) Advances in mechanical joining of magnesium. CIRP Annals – Manuf Technol 57(1):283–286
31. Lambiase F (2015) Clinch joining of heat-treatable aluminum AA6082-T6 alloy under warm conditions. J Mater Process Technol 225:421–432
32. Lambiase F, Di Llio A (2015) Mechanical clinching of metal-polymer joints. J Mater Process Technol 215:12–19
33. Lambiase F, Durante M, Di Llio A (2016) Fast joining of aluminum sheets with glass fiber reinforced polymer (GFRP) by mechanical clinching. J Mater Process Technol 236:241–251
34. Seok MY, Zhao Y, Lee JA, Mohamed RM, Al-Harbi LM, Al-Ghamdi MS, Singh G, Ramamurty U, Jang JI (2015) On the contributions of different micromechanics for enhancement in the strength of TI–6Al–4 V alloy upon B addition: a nanomechanical analysis. Mater Sci Eng A 694:123–127
35. Welsch G, Boyer R, Collings EW (1993) Materials properties handbook: titanium alloys. ASM international, Ohio, U.S.
36. He X, Zhang Y, Xing B, Gu F, Ball A (2015) Mechanical properties of extensible die clinched joints in titanium sheet materials. Mater Des 71:26–35
37. Fan X (2010) Heat treatment technology and practical technical manual, Second edn. Jiangsu Sci Technol Press, Jiangsu